



Masterarbeit MA 0000
Titel

Bearbeiter: Arda Buglagil

Betreuer: Prof.
Betreuer1
Betreuer2

Ausgabedatum: 01.04.2023
Abgabedatum: 30.09.2023

Ich versichere, dass ich die vorliegende Arbeit ohne fremde Hilfe und ohne Benutzung anderer als der angegebenen Quellen angefertigt habe und dass die Arbeit in gleicher oder ähnlicher Form noch keiner anderen Prüfungsbehörde vorgelegen hat und von dieser als Teil einer Prüfungsleistung angenommen wurde. Alle Ausführungen, die wörtlich oder sinngemäß übernommen wurden, sind als solche gekennzeichnet.

Ort, Datum

Unterschrift

Kurzzusammenfassung

— deutsche Kurzzusammenfassung —

Abstract

— englische Kurzzusammenfassung —

Inhaltsverzeichnis

| | |
|---|------------|
| Symbols | VII |
| 1 Introduction | 1 |
| 2 Grundlagen | 2 |
| 2.1 Aufzählungen | 2 |
| 2.2 Verlinkungen und Zitate | 2 |
| 2.2.1 Verlinkungen | 2 |
| 2.2.2 Zitate | 3 |
| 2.3 Einbinden von Bildern | 3 |
| 2.4 Gleichungen | 3 |
| 2.5 Tabellen | 5 |
| 3 Work Done | 6 |
| 3.1 Mapping Steering Mirror Coordinates to Target Plane Coordinates | 6 |
| 3.1.1 Computation of mirror normal vector (n_m) | 8 |
| 3.1.2 Computation of mirror coordinates (x, y) | 9 |
| 3.2 Position Error Measurement System | 10 |
| 3.2.1 Test results | 12 |
| 3.3 Mapping Depth Camera Coordinate System to Steering Mirror Coordinate System | 12 |
| 3.4 Calibration Procedure | 13 |
| 3.4.1 Visible Laser | 14 |
| 3.4.2 IR Laser | 15 |
| 3.4.3 Calibration Results | 18 |
| 3.5 Detection Algorithms | 18 |
| 3.5.1 ArUco | 18 |
| 3.5.2 Hough Circle Detector | 18 |
| 3.5.3 WHYCon | 20 |
| 3.5.4 Algorithm Performance Comparison | 20 |
| 3.6 Maximum distance of detection with different marker sizes | 21 |
| 3.7 Tracking Performance | 21 |

| | |
|------------------------------|-----------|
| 4 Zusammenfassung | 28 |
| A Anhang: Überschrift | 29 |
| Abbildungsverzeichnis | 31 |
| Tabellenverzeichnis | 33 |
| Literaturverzeichnis | 34 |

Symbols

| | |
|----------|---|
| P_0 | incoming beam origin |
| n_0 | incoming beam direction (unit vector) |
| M | mirror center |
| C | center of rotation |
| d | distance between M and C |
| n_m | mirror normal vector |
| P_1 | reflected beam origin |
| n_1 | reflected beam direction (unit vector) |
| D | distance between mirror center(C) and target plane |
| n_t | target plane normal vector |
| P_2 | the point reflected beam hits the target plane |
| α | rotation degree of the target plane with respect to steering mirror |

1 Introduction

— Introduction —

2 Grundlagen

2.1 Aufzählungen

L^AT_EX erlaubt viele verschiedene Formatierungen. Allein bei Aufzählungen sind *description* und *itemize* zu nennen:

Ein Stichpunkt mit Beschreibung

Noch ein Stichpunkt mit noch einer Beschreibung

- *kursiver Text*
- **fetter Text**
- normaler Text
- kleiner Text

2.2 Verlinkungen und Zitate

2.2.1 Verlinkungen

Dieses Kapitel hat die Nummer 2.2.1. Referenzen können das gesamte Dokument umfassen und zum Beispiel auch auf Bilder wie 2.2 verweisen.

Ein Link aus dem Dokument in das Internet ist mit dem Paket hyperref ebenfalls möglich:

<https://wch.github.io/latexsheet/>

Unter dieser Adresse findet sich ein gutes L^AT_EX Befehlsblatt!

2.2.2 Zitate

Zitate ergeben ebenfalls Verlinkungen ins Quellenverzeichnis [1] und [2, S.10].

Dies ist ein Zitat zum Test. Es ist an der Einrückung erkennbar. Bei langen Zitaten wird die automatische Einrückung der Folgezeilen sichtbar.

2.3 Einbinden von Bildern

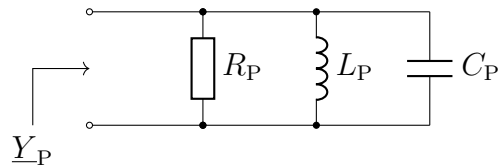


Abb. 2.1: Bild mit Tikz erstellt, Bildunterschrift einzeilig und zentriert.

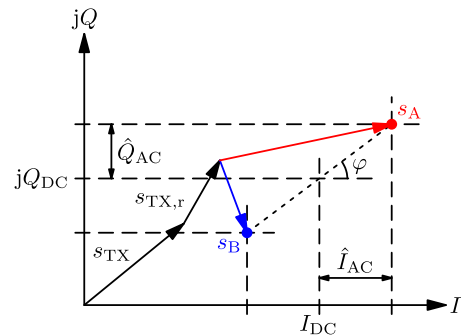


Abb. 2.2: Gewöhnliches Bild (hier pdf) und da dies eine zweizeilige Bildunterschrift ist, ist sie linksbündig und die zweite Zeile eingerückt.

2.4 Gleichungen

Gleichungen wie $a = b + c$ können in einem Fließtext als Inline-Formel auftreten oder als abgesetzte Formel:

$$x = \frac{1 + 2 + i}{2}. \quad (2.1)$$

Abgesetzte Formeln müssen in den Text eingefügt werden wie folgender Satz zeigt. Die Eulerformel, die man in der Form

$$e^{j\varphi} = \cos(\varphi) + j \sin(\varphi) \quad (2.2)$$

angeben kann, ist in vielen Formelsammlungen zu finden.

Bei den Formeln ist auf ISO-31 und DIN 1338 konformes Setzen zu achten. Dokumente hierzu findet man unter <http://www.moritz-nadler.de/formelsatz.pdf> und http://www.et.tu-dresden.de/ifa/fileadmin/user_upload/www_files/richtlinien_sa_da/auszug_din_1338.pdf

2.5 Tabellen

Tabellen können einfach mit der `tabular`-Umgebung aufgebaut werden.

Allerdings sind sie floats (sie ordnen sich automatisch an den besten Platz) und so oft irgendwo unterwegs. Diese Tabelle würde direkt über der Überschrift stehen, obwohl sie darunter definiert wurde. Dies kann mit `[!ht]` unterdrückt werden, was aber oft nicht sinnvoll ist (wegen den Regeln des Textsatzes). `[ht]` ist die abgeschwächte Version des Befehls und zu bevorzugen.

Tab. 2.1: Amateurfunkbänder (Auswahl)

| Band | Frequenzen | Nutzungsstatus |
|-------|---------------------|----------------|
| 80 m | 3,5 – 3,8 MHz | primär |
| 40 m | 7 – 7,1 MHz | primär |
| 20 m | 14 – 14,35 MHz | primär |
| 17 m | 18,068 – 18,168 MHz | primär |
| 15 m | 21 – 21,45 MHz | primär |
| 10 m | 28 – 29,7 MHz | primär |
| 2 m | 144 – 146 MHz | primär |
| 70 cm | 430 – 440 MHz | primär |
| 23 cm | 1240 – 1300 MHz | sekundär |
| 13 cm | 2320 – 2450 MHz | sekundär |

3 Work Done

3.1 Mapping Steering Mirror Coordinates to Target Plane Coordinates

To direct the laser beam MR-E-2 beam steering mirror is used. Laser beam is produced by a laser which is stationary. Laser is positioned to hit the steering mirror in the center. After the beam hits the mirror, it is directed to required position by adjusting the position of the mirror.

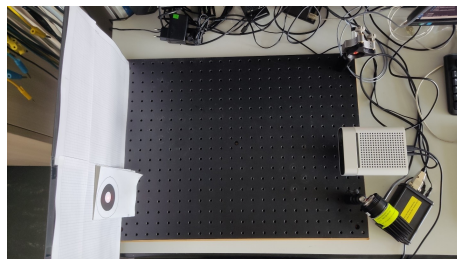
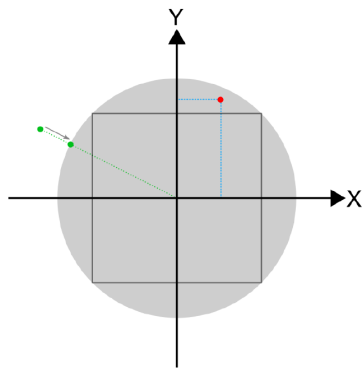
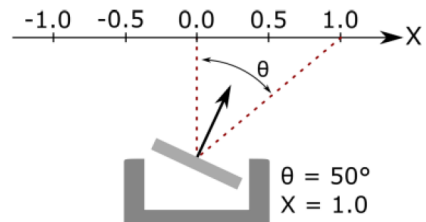
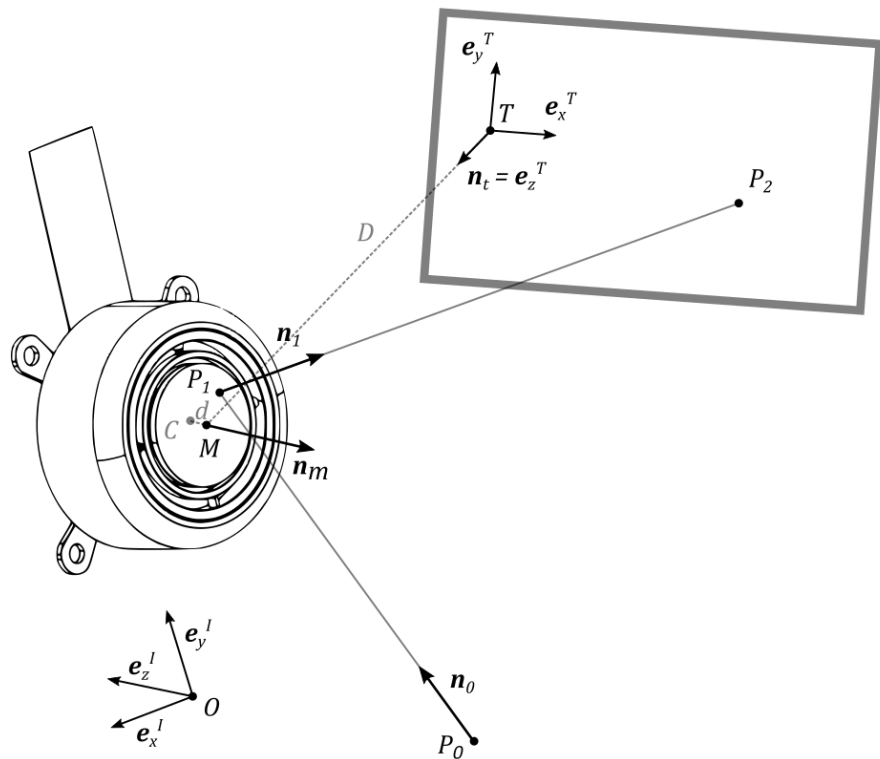


Abb. 3.1: Laser, depth camera, and beam steering mirror setup

Using the mirror to steer the laser beam requires a mapping from 3D world coordinate system to mirror coordinate system. The mapping calculates the required rotation of the mirror around its axes to direct the laser beam to intended 3D position. Mirror coordinate system is defined in [1] as in following figure.

The coordinate system is a Cartesian coordinate system with X and Y axes. Rotation of the mirror around its horizontal and vertical axes are expressed as x and y values. The range of both axes are $[-1, 1]$ interval. Mirror has maximum deflection angle of 25° . θ is the angle between incoming and reflected beam. $\theta = +50^\circ$ corresponds to +1 and $\theta = -50^\circ$ corresponds to -1. X and Y values are required to be inside a unit circle in order to be a valid point accessible by the mirror.

In the system setup used in experiments following configuration is used:

**Abb. 3.2:** Internal mirror coordinate system[1]**Abb. 3.3:** Relation between rotation of the mirror (θ) and the mirror coordinate (x) in X-axis[1]**Abb. 3.4:** Mirror coordinate system [1]

- $P_1 = M = C$
- $O = P_1 = M = C$
- $d = 0$
- Incoming ray is coming in y-z plane.

The conversion of coordinates on target plane (x_t, y_t) to mirror coordinates (x, y) is performed in two main steps. Firstly, the mirror normal (n_m) is calculated based on position of the laser, position of the target plane and (x_t, y_t) . In the next step, corresponding mirror coordinates (x, y) is calculated using n_m .

3.1.1 Computation of mirror normal vector (n_m)

There are 2 different frames of reference I and T. Reference frame I is centered around O . Its z-axis is aligned with $-n_m$ direction and its y-axis is aligned so that incoming laser beam propagates through yz plane. Reference frame T is centered around T. Its z-axis is aligned with n_t direction and its y-axis is aligned so that reflected laser beam propagates through yz plane. The transformation between frame of references is done with orthogonal transformation matrices A_{IT} and A_{TI} .

$$\begin{aligned}
 n_t^T &= \begin{bmatrix} 0 \\ 0 \\ 1 \end{bmatrix} & r_{OT}^T &= \begin{bmatrix} 0 \\ 0 \\ -D \end{bmatrix} \\
 r_{TP_2}^T &= \begin{bmatrix} x_t \\ y_t \\ 0 \end{bmatrix} & n_0^I &= \begin{bmatrix} 0 \\ 0 \\ 1 \end{bmatrix} \\
 A_{IT} &= \begin{bmatrix} 1 & 0 & 0 \\ 0 & \cos(\alpha) & -\sin(\alpha) \\ 0 & \sin(\alpha) & \cos(\alpha) \end{bmatrix}
 \end{aligned}$$

Mirror normal vector is calculated with following steps:

$$\begin{aligned}
n_t^I &= A_{IT} \cdot n_t^T \\
n_{OT}^I &= A_{IT} \cdot r_{OT}^T \\
r_{TP_2}^I &= A_{IT} \cdot r_{TP_2}^T \\
r_{OP_2}^I &= r_{OT}^T \cdot r_{TP_2}^I \\
n_1^I &= \text{normalize}(r_{OP_2}^I) \\
n_m^I &= \text{normalize}(n_1 - n_0)
\end{aligned}$$

3.1.2 Computation of mirror coordinates (x, y)

$$\begin{aligned}
r_C^I &= \begin{bmatrix} 0 \\ 0 \\ d \end{bmatrix} & N_0^I &= \begin{bmatrix} 0 \\ 0 \\ -1 \end{bmatrix} \\
n_t^T &= \begin{bmatrix} 0 \\ 0 \\ 1 \end{bmatrix} & r_{OT}^T &= \begin{bmatrix} 0 \\ 0 \\ -D \end{bmatrix} \\
A_{IT} &= \begin{bmatrix} 1 & 0 & 0 \\ 0 & 1 & 0 \\ 0 & 0 & 1 \end{bmatrix}
\end{aligned}$$

$$\begin{aligned}
t_1 &= \frac{(R_C^I - r_{OP_0}^I) \cdot n_m^I + d}{n_0^I \cdot n_m^I} \\
r_{OP_1}^I &= r_{OP_0}^I + t_1 \cdot n_0^I \\
n_1^I &= n_0^I - 2 \cdot (n_0^I \cdot n_m^I) \cdot n_m^I \\
t_2 &= \frac{(r_{OT}^T - r_{OP_1}^I) \cdot n_t^T}{n_1^I \cdot n_t^T} \\
r_{OP_2}^I &= r_{OP_1}^I + t_2 \cdot n_1^I \\
x &= \frac{r_{OP_2}^I[0]}{D \cdot \tan(50^\circ)} \\
y &= \frac{r_{OP_2}^I[1]}{D \cdot \tan(50^\circ)}
\end{aligned}$$

3.2 Position Error Measurement System



Abb. 3.5: Position error test setup

Measurements are done with a 2-dimensional servo motor system with a PM400 power meter attached. Measurements are performed by pointing the laser to a specified target position and then sweeping the power meter in a linear trajectory. Power recordings are recorded with recording times and plotted to find the instance with maximum power. The point with maximum power gives the center position of the laser. Power measurements are performed by a Python script which has a loop with a period of around 0.01s. This sampling period is not constant throughout the measurements and might deviate from 0.01s. For this reason, after the measurement, cubic interpolation is performed to get a uniformly sampled signal.

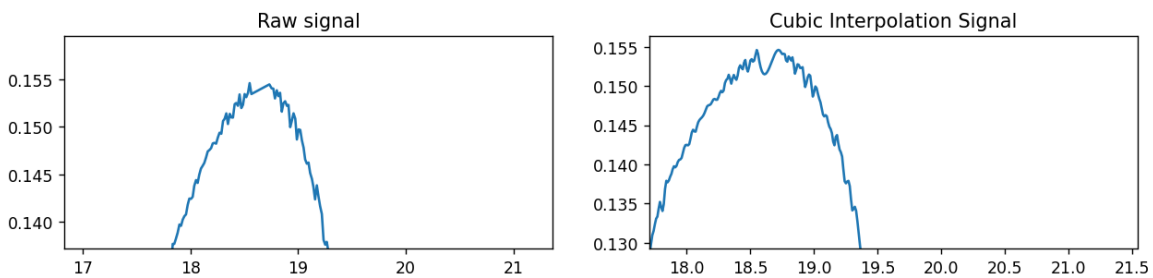


Abb. 3.6: Power(mW) - Position(mm) graphs for raw signal and cubic interpolation signal

Interpolation solves the nonuniform sampling problem. Obtained signal still has noise in it which might alter the maximum position. To remove the noise a low pass filter in the form of a moving average filter is applied. The figure below depicts the signal before and after the low pass filter. High-frequency noise components are removed from the signal while keeping the original signal mostly intact. This operation produced a smoother signal which is more suitable for peak finding operation.

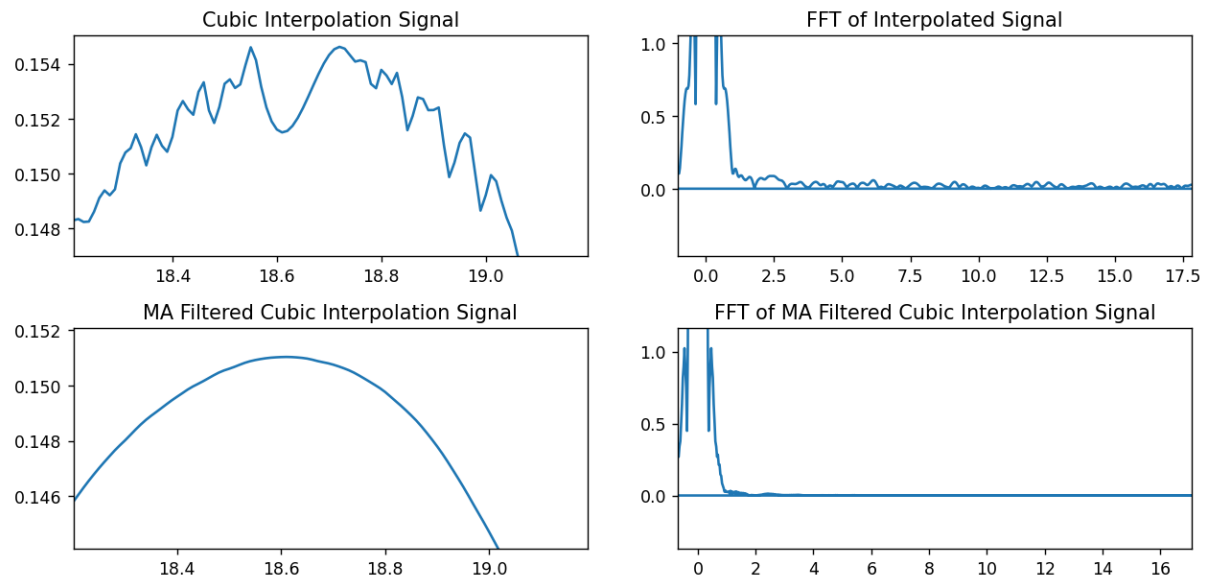


Abb. 3.7: Power(mW) - Position(mm) graphs for raw signal and cubic interpolation signal

The recorded power signal is plotted with respect to distance in order to find the position of the laser's center. This method gives the position of the laser relative to the initial position of the servo motor. The figure below shows the power levels with respect to time and position. Position with maximum power is written in the fourth graph in millimeters.

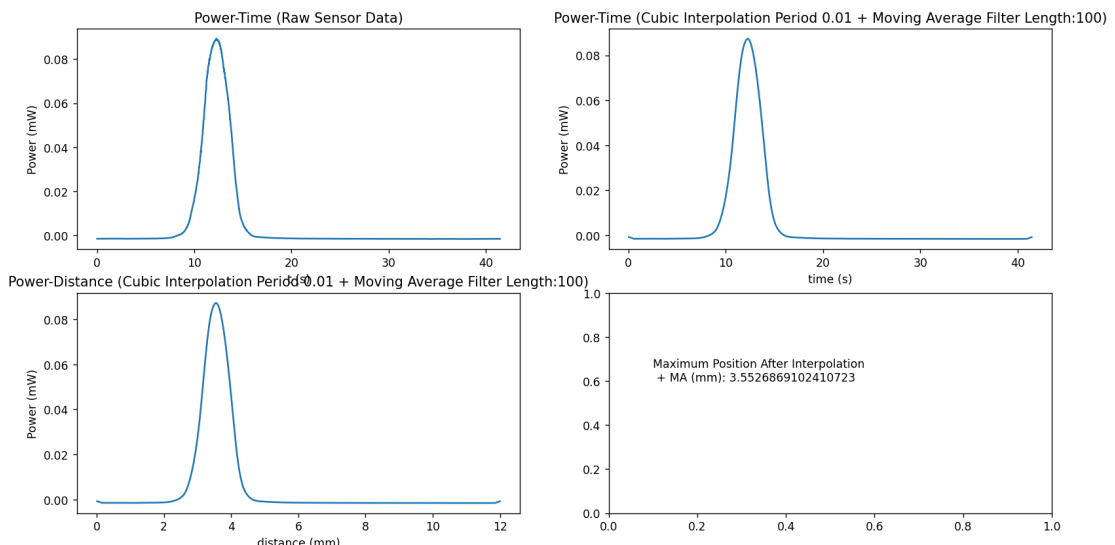


Abb. 3.8: Power(mW) - Position(mm) graphs for raw signal and cubic interpolation signal

Measurements are performed with different parameters such as the distance between the mirror and target plane, different sweep locations.

3.2.1 Test results

The coordinate systems that are used in the steering mirror and the depth camera don't coincide. They are rotated and translated versions of each other. A point in camera coordinate system, c , can be transformed into a point in mirror coordinate system, m , with the following mapping:

3.3 Mapping Depth Camera Coordinate System to Steering Mirror Coordinate System

The coordinate systems that are used in the steering mirror and the depth camera don't coincide. They are rotated and translated versions of each other. A point in camera coordinate system, c , can be transformed into a point in mirror coordinate system, m , with the following mapping:

$$m = Rc + t$$

R is 3×3 an orthogonal rotation matrix and t is a 3×1 translation vector. Optimal R and t are found by the following algorithm [2] [3] [4]: R is an orthogonal rotation matrix and t is a translation vector. Optimal R and t are found by the following algorithm [2] [3] [4]:

To find the rotation matrix R ,

$$\begin{aligned} H &= (A - m_A)(B - m_B)^T \\ U, S, V^T &= SVD(H) \\ R &= VU^T \end{aligned}$$

To find translation vector t ,

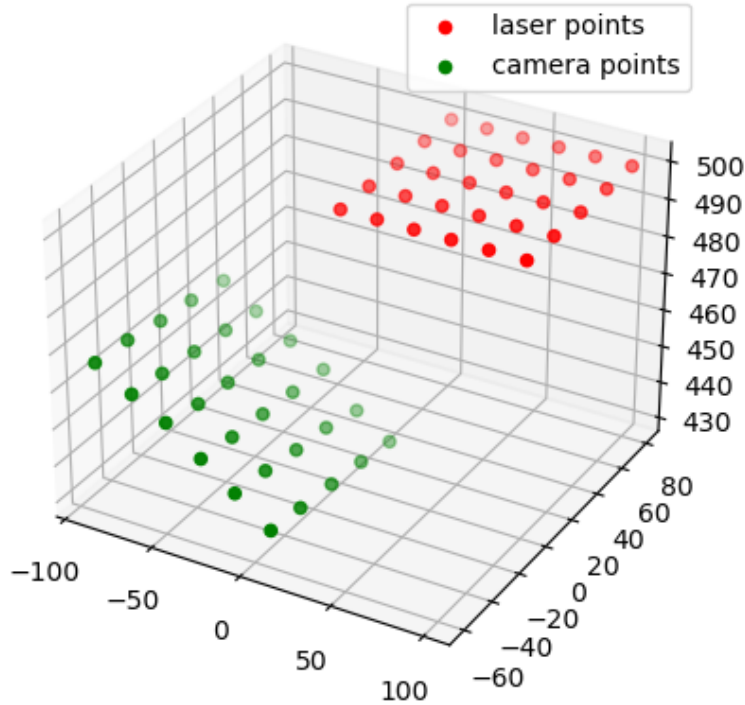


Abb. 3.9: Recording of the same points in steering mirror and depth camera coordinate systems

$$t = m_B - Rm_A$$

Optimal transformation maps each point in camera coordinate system to a point in mirror coordinate system. After the mapping mirror points and camera points are almost aligned as shown in Figure 8. With this mapping, any point recorded by depth camera can be transformed into a point which can be used by the mirror controller.

3.4 Calibration Procedure

Calibration of the system is done in order to coordinate depth camera and mirror together. Both steering mirror and depth camera have their own coordinate systems. The relationship between these coordinate systems is unknown which makes them unable to

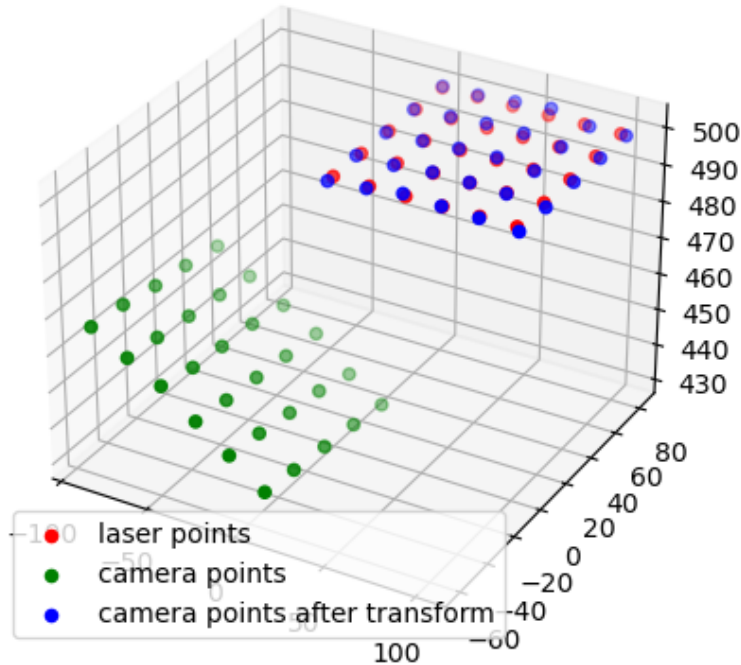


Abb. 3.10: Camera points after the transformation

perform tasks together. The main objective of the calibration is to find the rotation and translation of the coordinate systems relative to each other. For this purpose, the optimal R and t finding algorithm discussed in previous chapter is used. Calibration procedure is responsible for obtaining point pairs consisting of a point in depth camera coordinate system and its corresponding point in steering mirror coordinate system. After the collection of the dataset, the mapping is computed and saved for later usage. Point pair collection operation depends on the type of laser used in the system. For easier testing a visible laser is used. However, in the end system an IR laser is used. Using IR laser restricts the usage of camera since it is not visible by camera sensor. IR laser requires IR light intensity sensors to detect and a different calibration procedure than visible laser.

3.4.1 Visible Laser

The laser is pointed at 30 different positions in a plane 560 mm away from the mirror center. These points are recorded as mirror points B. Each laser position is extrac-

ted from the color images by using Hough Circle Detection algorithm. Once 2D pixel coordinates are found they are converted to 3D coordinates by Kinect Azure SDK's `k4a::calibration::convert_2d_to_3d` [5] function. Extracted 3D depth camera points are named A. Points A and B are formed into matrices with shape 3xN. Finally, algorithm 1 is used to find R and t matrices

3.4.2 IR Laser

IR laser requires different calibration method from the visible laser. Point patching operation is done via laser intensity sensors. The sensor setup used to detect positions is in figure below. 3 sensors generate analog output signals based on the intensity of light hitting them. The analog signal is captured by ADCs on a Raspberry Pi Pico board and transmitted to host computer via USB. –add sensor picture While the sensor is recording the signal intensity, laser scans the area near the sensor position based on an initial sensor position estimate in terms of a 3D coordinate. Each signal point is plotted with respect to position of the laser at the time of recording. As a result, an intensity profile is generated. The maximum intensity level of this profile is chosen as the sensor position. This process is performed by all three sensors, and 3 different images are generated. In each image a peak intensity is observed, and it is marked as that specific sensor's position.

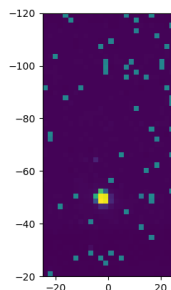


Abb. 3.11: Rough sensor image.

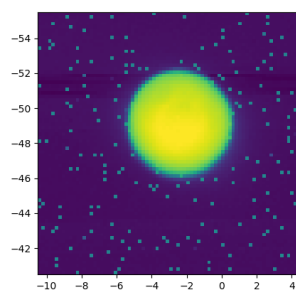


Abb. 3.12: Fine sensor image.

3 3D coordinates generated are not exact coordinates due to the initial position estimate. The x and y positions determined by scanning the laser are valid if and only if the initial distance between mirror center and target plane is correct. Since this won't be the case for most cases, found points should be used to calculate the real distance between mirror center and target plane.

To calculate the distance between mirror center and target plane, the geometry of the sensors is used. Sensors are placed on top of each other as in Figure 9 and the plate holding the sensors is placed perpendicular to ground. This configuration places all the sensors at the same distance from mirror center in the z direction. Using this constraint, the distance between sensors and mirror center in z direction is calculated:

$$\begin{aligned} d1 &= |M1 \cdot \frac{z2}{z1} - M2 \cdot \frac{z2}{z1}| & d2 &= |M2 \cdot \frac{z2}{z1} - M3 \cdot \frac{z2}{z1}| & d3 &= |M1 \cdot \frac{z2}{z1} - M3 \cdot \frac{z2}{z1}| \\ z2 &= \frac{d1 \cdot z1}{|M1 - M2|} & z2 &= \frac{d2 \cdot z1}{|M2 - M3|} & z2 &= \frac{d3 \cdot z1}{|M1 - M3|} \end{aligned}$$

With the $z2$ distance obtained, previous 3D coordinates are updated and they are saved as mirror points B. The next step is to find the sensor positions with the depth camera and to obtain depth camera points A. To localize the sensors, the marker pattern in figure below is attached to the sensor plate. Each circular fiducial marker is localized using WHYCon algorithm (will be discussed later). Two unit vectors are extracted from the 3D coordinates of markers.

$$u_l = B - A$$

$$u_d = C - A$$

Unit vectors u_l and u_d are used to locate the 3D position of the sensors. This is possible since markers and the marker pattern are on the same plane. Found points are recorded as depth camera points A. Points A and B are formed into matrices with shape $3 \times N$. Finally, algorithm 1 is used to find R and t matrices.

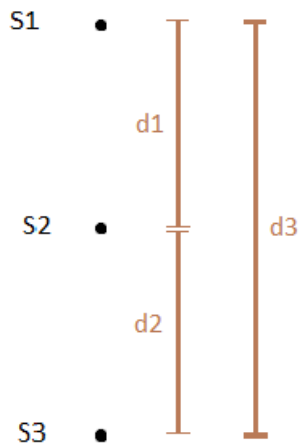


Abb. 3.13: Sensor positions (S_1, S_2, S_3), detected sensor positions (M_1, M_2, M_3) and steering mirror position (O) from camera view.

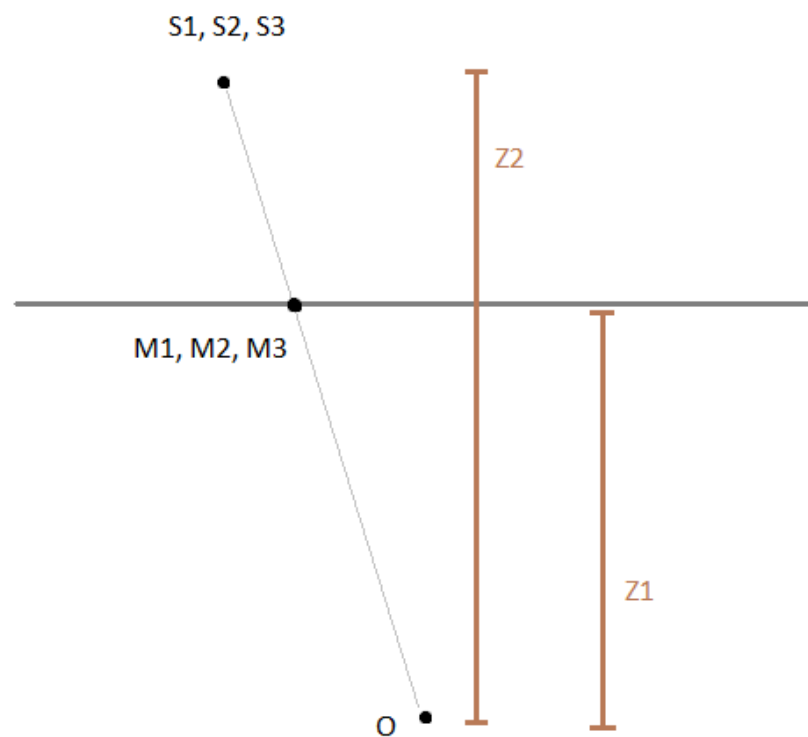


Abb. 3.14: Sensor positions (S_1, S_2, S_3), detected sensor positions (M_1, M_2, M_3) and steering mirror position (O) from top view.

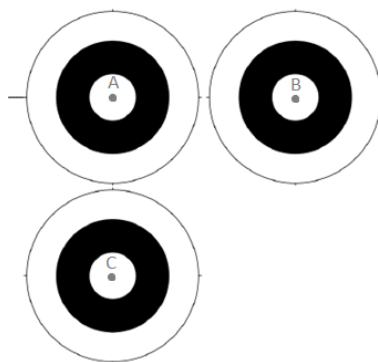


Abb. 3.15: Localization marker pattern with WHYCon marker

3.4.3 Calibration Results

3.5 Detection Algorithms

Position estimation is the first step to tracking the position of the body. One of the most common approaches to this problem is usage of visual markers. A visual marker can be distinguished from the environment without too much difficulty due to its characteristics. For the project 3 different algorithms are tested: ArUco, Hough Circle Detector, and WHYCon. Detection algorithms are evaluated based on their processing times in order to choose the best option for the system.

3.5.1 ArUco

ArUco is a popular binary square fiducial marker used for absolute pose estimation. ArUco markers are black square shapes with an inner grid structure to encode a binary code. The binary code is used to identify the markers and distinguish multiple markers inside the same camera view. Due to the encoding, Aruco markers are not easily detected from far distances. [6]

3.5.2 Hough Circle Detector

-TODO

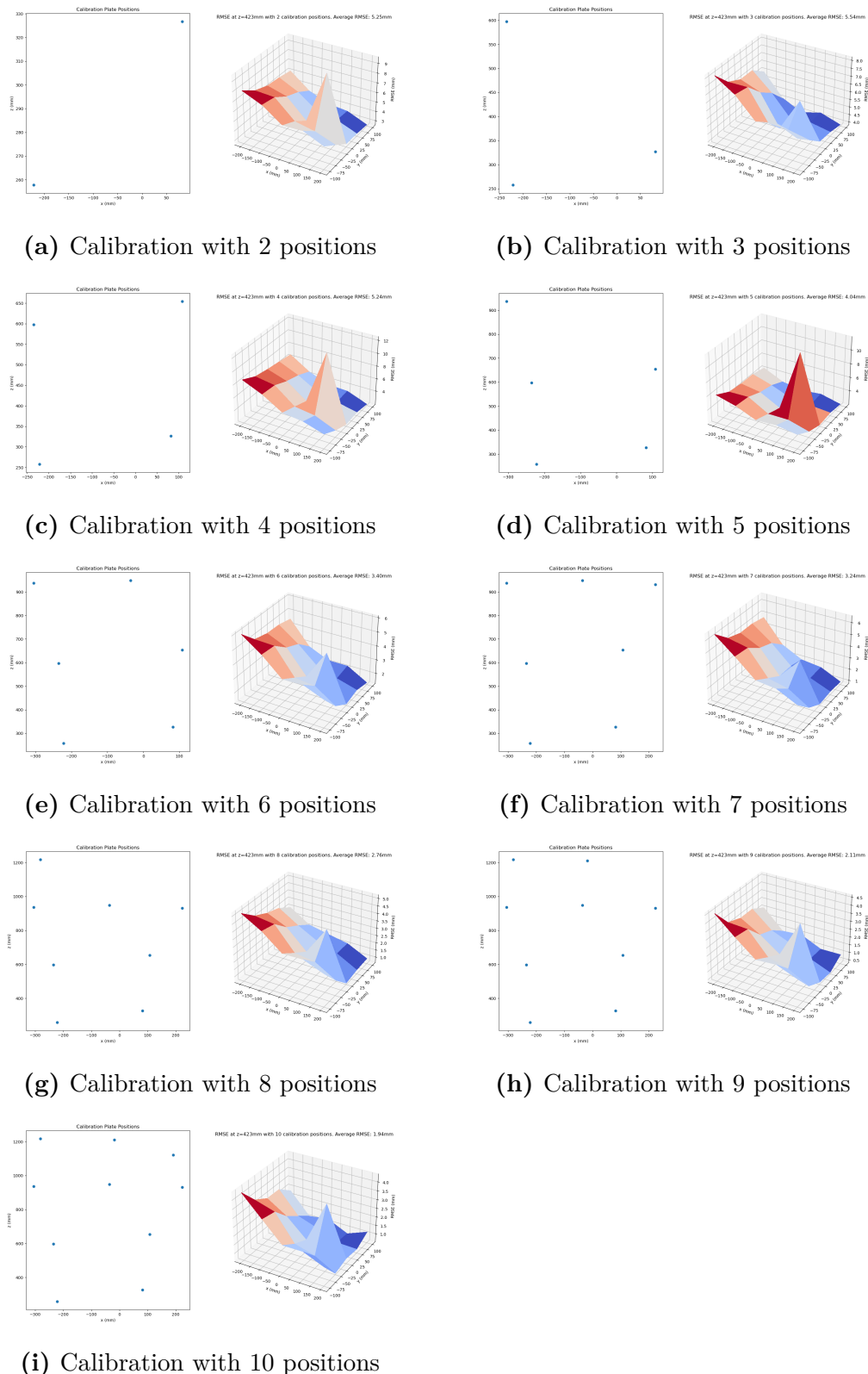


Abb. 3.16: Calibration plate positions and calibration error at each x-y position at a distance of $z=423\text{mm}$.

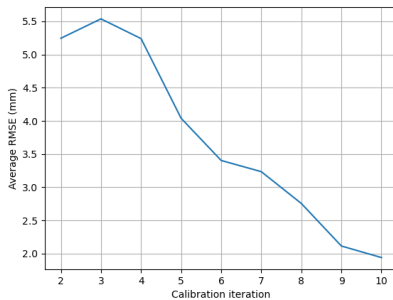


Abb. 3.17: Calibration RMSE scores with respect to number of calibration points (calibration iterations) used



Abb. 3.18: ArUco marker with ids 0 up to 3 [6]

3.5.3 WHYCon

WHYCon is an open-source marker-based localization system. It is highly computationally efficient. [7] WHYCon doesn't provide ant identification information, its marker consists of black and white concentric circles. Due to its simplicity, it can be identified easily and it requires low computational resources. During implementation, only option that was able to run on a Windows machine was a C++ repository. To connect the algorithm to rest of the system, Python bindings were implemented using Pybind11.

3.5.4 Algorithm Performance Comparison

All of the algorithms are run on the same computer with Intel i7. Based on the runtimes WHYCon is the most performant algorithm. ArUco has similar performance with 4ms, but in case of movement and bad lighting conditions the runtime can increase up to 30ms. With a 30ms runtime the algorithm is not suitable for real time tracking. Hough Circle Detector also has good runtime, but WHYCon outperforms it. Due to its performance, WHYCon is used in the system.

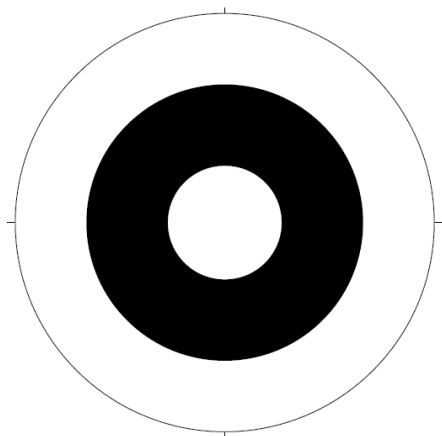


Abb. 3.19: WHYCon marker [8]

3.6 Maximum distance of detection with different marker sizes

Maximum distance detection test is performed with WHYCon detection algorithm. Tests are performed with distances 400mm, 600mm, 800mm away from steering mirror center. Tests are repeated for 720p and 1080p image resolutions.

3.7 Tracking Performance

-TODO

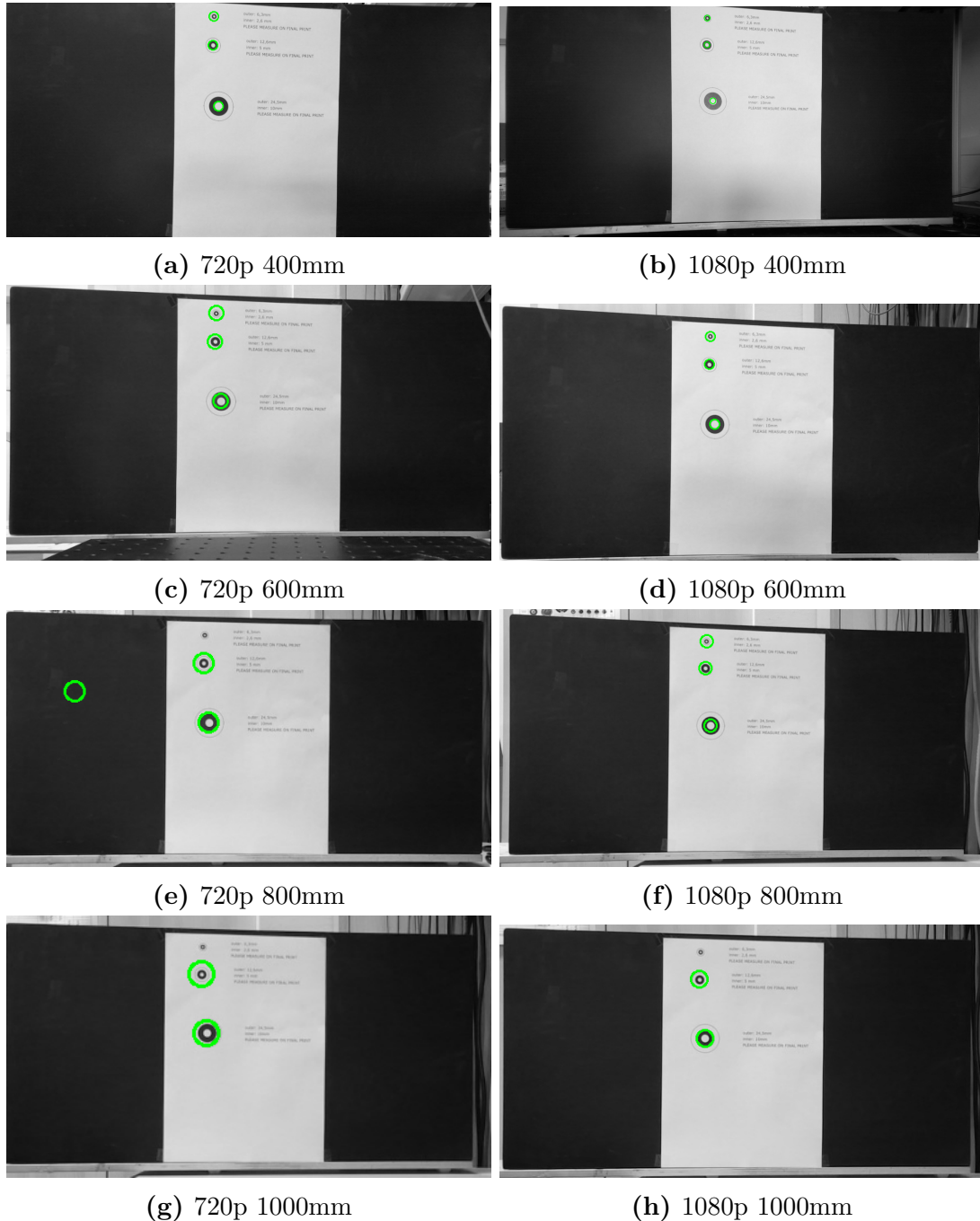


Abb. 3.20: Detection results of WHYCon marker at different distances and different resolutions

Tab. 3.1: Distance between mirror and target plane is set to 410mm. Actual distance between mirror and target plane is 425mm.

| Mirror Input x | Mirror Input y | Peak Power Position | Relative Distance |
|----------------|----------------|---------------------|-------------------|
| -3 mm | -5 mm | 2,322 mm | -3,096 mm |
| -2,5 mm | -5 mm | 2,853 mm | -2,565 mm |
| -2 mm | -5 mm | 3,372 mm | -2,046 mm |
| -1,5 mm | -5 mm | 3,868 mm | -1,550 mm |
| -1 mm | -5 mm | 4,392 mm | -1,026 mm |
| -0,5 mm | -5 mm | 4,905 mm | -0,513 mm |
| 0 mm | -5 mm | 5,418 mm | 0 mm |
| 0,5 mm | -5 mm | 5,921 mm | 0,503 mm |
| 1 mm | -5 mm | 6,446 mm | 1,028 mm |
| 1,5 mm | -5 mm | 6,923 mm | 1,505 mm |
| 2 mm | -5 mm | 7,427 mm | 2,009 mm |
| 2,5 mm | -5 mm | 7,937 mm | 2,519 mm |
| 3 mm | -5 mm | 8,452 mm | 3,034 mm |
| -3 mm | 0 mm | 2,278 mm | -3,089 mm |
| -2,5 mm | 0 mm | 2,792 mm | -2,575 mm |
| -2 mm | 0 mm | 3,311 mm | -2,056 mm |
| -1,5 mm | 0 mm | 3,829 mm | -1,538 mm |
| -1 mm | 0 mm | 4,327 mm | -1,040 mm |
| -0,5 mm | 0 mm | 4,860 mm | -0,507 mm |
| 0 mm | 0 mm | 5,367 mm | 0 mm |
| 0,5 mm | 0 mm | 5,878 mm | 0,511 mm |
| 1 mm | 0 mm | 6,379 mm | 1,012 mm |
| 1,5 mm | 0 mm | 6,880 mm | 1,513 mm |
| 2 mm | 0 mm | 7,392 mm | 2,025 mm |
| 2,5 mm | 0 mm | 7,880 mm | 2,513 mm |
| 3 mm | 0 mm | 8,390 mm | 3,023 mm |
| -3 mm | 5 mm | 2,391 mm | -3,097 mm |
| -2,5 mm | 5 mm | 2,909 mm | -2,579 mm |
| -2 mm | 5 mm | 3,424 mm | -2,064 mm |
| -1,5 mm | 5 mm | 3,949 mm | -1,539 mm |
| -1 mm | 5 mm | 4,468 mm | -1,020 mm |
| -0,5 mm | 5 mm | 4,974 mm | -0,514 mm |
| 0 mm | 5 mm | 5,488 mm | 0 mm |
| 0,5 mm | 5 mm | 6,013 mm | 0,525 mm |
| 1 mm | 5 mm | 6,534 mm | 1,046 mm |
| 1,5 mm | 5 mm | 7,042 mm | 1,554 mm |
| 2 mm | 5 mm | 7,547 mm | 2,059 mm |
| 2,5 mm | 5 mm | 8,052 mm | 2,564 mm |
| 3 mm | 5 mm | 8,561 mm | 3,073 mm |

Tab. 3.2: Distance between mirror and target plane is set to 425mm. Actual distance between mirror and target plane is 425mm.

| Mirror Input x | Mirror Input y | Peak Power Position | Relative Distance |
|----------------|----------------|---------------------|-------------------|
| -3 mm | -5 mm | 6,723 mm | -2,999 mm |
| -2,5 mm | -5 mm | 7,225 mm | -2,497 mm |
| -2 mm | -5 mm | 7,727 mm | -1,995 mm |
| -1,5 mm | -5 mm | 8,218 mm | -1,504 mm |
| -1 mm | -5 mm | 8,716 mm | -1,007 mm |
| -0,5 mm | -5 mm | 9,228 mm | -0,494 mm |
| 0 mm | -5 mm | 9,722 mm | 0,0 mm |
| 0,5 mm | -5 mm | 10,212 mm | 0,49 mm |
| 1 mm | -5 mm | 10,695 mm | 0,973 mm |
| 1,5 mm | -5 mm | 11,191 mm | 1,469 mm |
| 2 mm | -5 mm | 11,673 mm | 1,951 mm |
| 2,5 mm | -5 mm | 12,151 mm | 2,429 mm |
| 3 mm | -5 mm | 12,653 mm | 2,931 mm |
| -3 mm | 0 mm | 6,788 mm | -2,956 mm |
| -2,5 mm | 0 mm | 7,275 mm | -2,469 mm |
| -2 mm | 0 mm | 7,777 mm | -1,967 mm |
| -1,5 mm | 0 mm | 8,289 mm | -1,455 mm |
| -1 mm | 0 mm | 8,758 mm | -0,986 mm |
| -0,5 mm | 0 mm | 9,248 mm | -0,496 mm |
| 0 mm | 0 mm | 9,744 mm | 0,0 mm |
| 0,5 mm | 0 mm | 10,225 mm | 0,481 mm |
| 1 mm | 0 mm | 10,711 mm | 0,967 mm |
| 1,5 mm | 0 mm | 11,207 mm | 1,463 mm |
| 2 mm | 0 mm | 11,666 mm | 1,922 mm |
| 2,5 mm | 0 mm | 12,156 mm | 2,412 mm |
| 3 mm | 0 mm | 12,654 mm | 2,91 mm |
| -3 mm | 5 mm | 6,849 mm | -2,978 mm |
| -2,5 mm | 5 mm | 7,364 mm | -2,463 mm |
| -2 mm | 5 mm | 7,867 mm | -1,959 mm |
| -1,5 mm | 5 mm | 8,359 mm | -1,468 mm |
| -1 mm | 5 mm | 8,843 mm | -0,984 mm |
| -0,5 mm | 5 mm | 9,34 mm | -0,487 mm |
| 0 mm | 5 mm | 9,826 mm | 0,0 mm |
| 0,5 mm | 5 mm | 10,308 mm | 0,481 mm |
| 1 mm | 5 mm | 10,824 mm | 0,998 mm |
| 1,5 mm | 5 mm | 11,304 mm | 1,478 mm |
| 2 mm | 5 mm | 11,793 mm | 1,967 mm |
| 2,5 mm | 5 mm | 12,279 mm | 2,453 mm |
| 3 mm | 5 mm | 12,781 mm | 2,954 mm |

Tab. 3.3: Distance between mirror and target plane is set to 210mm. Actual distance between mirror and target plane is 225mm.

| Mirror Input x | Mirror Input y | Peak Power Position | Relative Distance |
|----------------|----------------|---------------------|-------------------|
| -3 mm | -5 mm | 6,723 mm | -2,999 mm |
| -2,5 mm | -5 mm | 7,225 mm | -2,497 mm |
| -2 mm | -5 mm | 7,727 mm | -1,995 mm |
| -1,5 mm | -5 mm | 8,218 mm | -1,504 mm |
| -1 mm | -5 mm | 8,716 mm | -1,007 mm |
| -0,5 mm | -5 mm | 9,228 mm | -0,494 mm |
| 0 mm | -5 mm | 9,722 mm | 0,0 mm |
| 0,5 mm | -5 mm | 10,212 mm | 0,49 mm |
| 1 mm | -5 mm | 10,695 mm | 0,973 mm |
| 1,5 mm | -5 mm | 11,191 mm | 1,469 mm |
| 2 mm | -5 mm | 11,673 mm | 1,951 mm |
| 2,5 mm | -5 mm | 12,151 mm | 2,429 mm |
| 3 mm | -5 mm | 12,653 mm | 2,931 mm |
| -3 mm | 0 mm | 6,788 mm | -2,956 mm |
| -2,5 mm | 0 mm | 7,275 mm | -2,469 mm |
| -2 mm | 0 mm | 7,777 mm | -1,967 mm |
| -1,5 mm | 0 mm | 8,289 mm | -1,455 mm |
| -1 mm | 0 mm | 8,758 mm | -0,986 mm |
| -0,5 mm | 0 mm | 9,248 mm | -0,496 mm |
| 0 mm | 0 mm | 9,744 mm | 0,0 mm |
| 0,5 mm | 0 mm | 10,225 mm | 0,481 mm |
| 1 mm | 0 mm | 10,711 mm | 0,967 mm |
| 1,5 mm | 0 mm | 11,207 mm | 1,463 mm |
| 2 mm | 0 mm | 11,666 mm | 1,922 mm |
| 2,5 mm | 0 mm | 12,156 mm | 2,412 mm |
| 3 mm | 0 mm | 12,654 mm | 2,91 mm |
| -3 mm | 5 mm | 6,849 mm | -2,978 mm |
| -2,5 mm | 5 mm | 7,364 mm | -2,463 mm |
| -2 mm | 5 mm | 7,867 mm | -1,959 mm |
| -1,5 mm | 5 mm | 8,359 mm | -1,468 mm |
| -1 mm | 5 mm | 8,843 mm | -0,984 mm |
| -0,5 mm | 5 mm | 9,34 mm | -0,487 mm |
| 0 mm | 5 mm | 9,826 mm | 0,0 mm |
| 0,5 mm | 5 mm | 10,308 mm | 0,481 mm |
| 1 mm | 5 mm | 10,824 mm | 0,998 mm |
| 1,5 mm | 5 mm | 11,304 mm | 1,478 mm |
| 2 mm | 5 mm | 11,793 mm | 1,967 mm |
| 2,5 mm | 5 mm | 12,279 mm | 2,453 mm |
| 3 mm | 5 mm | 12,781 mm | 2,954 mm |

Tab. 3.4: Distance between mirror and target plane is set to 225mm. Actual distance between mirror and target plane is 225mm.

| Mirror Input x | Mirror Input y | Peak Power Position | Relative Distance |
|----------------|----------------|---------------------|-------------------|
| -3 mm | -5 mm | 4,985 mm | -3,044 mm |
| -2,5 mm | -5 mm | 5,503 mm | -2,526 mm |
| -2 mm | -5 mm | 6,007 mm | -2,023 mm |
| -1,5 mm | -5 mm | 6,505 mm | -1,524 mm |
| -1 mm | -5 mm | 7,034 mm | -0,995 mm |
| -0,5 mm | -5 mm | 7,536 mm | -0,494 mm |
| 0 mm | -5 mm | 8,029 mm | 0,0 mm |
| 0,5 mm | -5 mm | 8,539 mm | 0,509 mm |
| 1 mm | -5 mm | 9,045 mm | 1,016 mm |
| 1,5 mm | -5 mm | 9,546 mm | 1,517 mm |
| 2 mm | -5 mm | 10,045 mm | 2,015 mm |
| 2,5 mm | -5 mm | 10,529 mm | 2,499 mm |
| 3 mm | -5 mm | 11,009 mm | 2,98 mm |
| -3 mm | 0 mm | 4,989 mm | -2,992 mm |
| -2,5 mm | 0 mm | 5,493 mm | -2,488 mm |
| -2 mm | 0 mm | 5,999 mm | -1,982 mm |
| -1,5 mm | 0 mm | 6,49 mm | -1,491 mm |
| -1 mm | 0 mm | 6,998 mm | -0,984 mm |
| -0,5 mm | 0 mm | 7,459 mm | -0,523 mm |
| 0 mm | 0 mm | 7,981 mm | 0,0 mm |
| 0,5 mm | 0 mm | 8,461 mm | 0,479 mm |
| 1 mm | 0 mm | 8,952 mm | 0,971 mm |
| 1,5 mm | 0 mm | 9,485 mm | 1,503 mm |
| 2 mm | 0 mm | 9,976 mm | 1,994 mm |
| 2,5 mm | 0 mm | 10,464 mm | 2,483 mm |
| 3 mm | 0 mm | 10,956 mm | 2,975 mm |
| -3 mm | 5 mm | 5,156 mm | -2,982 mm |
| -2,5 mm | 5 mm | 5,664 mm | -2,475 mm |
| -2 mm | 5 mm | 6,153 mm | -1,986 mm |
| -1,5 mm | 5 mm | 6,649 mm | -1,49 mm |
| -1 mm | 5 mm | 7,154 mm | -0,985 mm |
| -0,5 mm | 5 mm | 7,64 mm | -0,498 mm |
| 0 mm | 5 mm | 8,138 mm | 0,0 mm |
| 0,5 mm | 5 mm | 8,634 mm | 0,496 mm |
| 1 mm | 5 mm | 9,126 mm | 0,988 mm |
| 1,5 mm | 5 mm | 9,635 mm | 1,497 mm |
| 2 mm | 5 mm | 10,126 mm | 1,988 mm |
| 2,5 mm | 5 mm | 10,609 mm | 2,47 mm |
| 3 mm | 5 mm | 11,103 mm | 2,965 mm |

Tab. 3.5: Detection Algorithm Performances

| Algorithm | Runtime (ms) |
|-----------------------|--------------|
| ArUco | 4-30 |
| WHYCon | 2-3 |
| Hough Circle Detector | 8-10 |

Tab. 3.6: Runtime of different code sections

| Code Sections | Elapsed Time (ms) |
|--|-------------------|
| Capturing Color Image | 3 |
| Marker Detection | 2 |
| Transforming Depth Image to Color Camera's Coordinate System | 15 |
| 3D to mirror coordinate conversion | 1 |
| Mirror Adjustment | 2 |
| Total Time | 23 |

4 Zusammenfassung

— Zusammenfassung —

A Anhang: Überschrift

— Anhang —

Abbildungsverzeichnis

| | | |
|------|--|----|
| 2.1 | Bild mit Tikz erstellt, Bildunterschrift einzeilig und zentriert. | 3 |
| 2.2 | Gewöhnliches Bild (hier pdf) und da dies eine zweizeilige Bildunterschrift ist, ist sie linksbündig und die zweite Zeile eingerückt. | 3 |
| 3.1 | Laser, depth camera, and beam steering mirror setup | 6 |
| 3.2 | Internal mirror coordinate system[1] | 7 |
| 3.3 | Relation between rotation of the mirror (θ) and the mirror coordinate (x) in X-axis[1] | 7 |
| 3.4 | Mirror coordinate system [1] | 7 |
| 3.5 | Position error test setup | 10 |
| 3.6 | Power(mW) - Position(mm) graphs for raw signal and cubic interpolation signal | 10 |
| 3.7 | Power(mW) - Position(mm) graphs for raw signal and cubic interpolation signal | 11 |
| 3.8 | Power(mW) - Position(mm) graphs for raw signal and cubic interpolation signal | 11 |
| 3.9 | Recording of the same points in steering mirror and depth camera coordinate systems | 13 |
| 3.10 | Camera points after the transformation | 14 |
| 3.11 | Rough sensor image. | 15 |
| 3.12 | Fine sensor image. | 15 |
| 3.13 | Sensor positions (S1, S2, S3), detected sensor positions (M1, M2, M3) and steering mirror position (O) from camera view. | 17 |
| 3.14 | Sensor positions (S1, S2, S3), detected sensor positions (M1, M2, M3) and steering mirror position (O) from top view. | 17 |
| 3.15 | Localization marker pattern with WHYCon marker | 18 |
| 3.16 | Calibration plate positions and calibration error at each x-y position at a distance of z=423mm. | 19 |

| | |
|--|----|
| 3.17 Calibration RMSE scores with respect to number of calibration points (calibration iterations) used | 20 |
| 3.18 ArUco marker with ids 0 up to 3 [6] | 20 |
| 3.19 WHYCon marker [8] | 21 |
| 3.20 Detection results of WHYCon marker at different distances and different resolutions | 22 |

Tabellenverzeichnis

| | | |
|-----|---|----|
| 2.1 | Amateurfunkbänder (Auswahl) | 5 |
| 3.1 | Distance between mirror and target plane is set to 410mm. Actual distance between mirror and target plane is 425mm. | 23 |
| 3.2 | Distance between mirror and target plane is set to 425mm. Actual distance between mirror and target plane is 425mm. | 24 |
| 3.3 | Distance between mirror and target plane is set to 210mm. Actual distance between mirror and target plane is 225mm. | 25 |
| 3.4 | Distance between mirror and target plane is set to 225mm. Actual distance between mirror and target plane is 225mm. | 26 |
| 3.5 | Detection Algorithm Performances | 27 |
| 3.6 | Runtime of different code sections | 27 |

Literaturverzeichnis

- [1] FINKENZELLER, K.: *RFID-Handbuch: Grundlagen und praktische Anwendungen von Transpondern, kontaktlosen Chipkarten und NFC.* 7. Auflage. Carl Hanser Verlag GmbH & Company KG, 2015
- [2] TIETZE, U. ; SCHENK, C. ; GRAMM, E.: *Halbleiter-Schaltungstechnik.* 13. Auflage. Springer-Verlag Berlin Heidelberg, 2010